◄— Previous section
◄— Volume contents

Geochemistry of Volcanic Rocks in the Marysvale Volcanic Field, West-Central Utah

By Charles G. Cunningham, Daniel M. Unruh, Thomas A. Steven, Peter D. Rowley, Charles W. Naeser, Harald H. Mehnert, Carl E. Hedge, and Kenneth R. Ludwig[1]

CONTENTS

FIGURES

TABLE

ABSTRACT

Igneous activity in the Marysvale volcanic field of west-central Utah occurred in three episodes. The first took place 34–22 Ma and was dominated by calc-alkaline, intermediate composition rocks of the Bullion Canyon Volcanics and Mount Dutton Formations. The e_{Nd} increased with time, reflecting decreasing crustal interaction with time. The second episode, 23–14 Ma, was dominated by an alkali-rhyolite and basalt (bimodal) assemblage. The similarity in isotopic ratios, together with a change to alkali rhyolites, is interpreted to be due to derivation of the nearly eutectic rhyolites by remelting the batholithic rocks that previously fed the Bullion Canyon volcanoes. Potassium-rich mafic rocks were erupted early in the second episode and were followed by more normal basalts. The third episode, 9–5 Ma, was also characterized by a bimodal assemblage of volcanic rocks. The highly variable isotopic ratios of the rhyolites indicate derivation from variable sources, reflecting episodic intervals of extensional tectonics.

[1]Berkeley Geochronology Center, 2455 Ridge Road, Berkeley, CA 94709.

Igneous activity and associated mineralization in the Marysvale volcanic field along the west side of the Colorado Plateau in west-central Utah occurred mainly during three episodes: ≈34–22 Ma, 23–14 Ma, and 9–5 Ma. In the first episode, during a regime of tectonic convergence, two contrasting suites of rocks were erupted concurrently: (1) poorly evolved, crystal-poor, pyroxene-plagioclase-bearing andesitic rocks, called the Mount Dutton Formation, from deep sources along the southern flank of the volcanic field, and (2) crystal-rich, biotite-hornblende-plagioclase-bearing dacitic rocks, called the Bullion Canyon Volcanics, from an east-northeast-trending shallow batholith under the middle of the field (Rowley and others, 1979, 1994; Steven and others, 1979, 1990; Steven, Rowley, and Cunningham, 1984; Cunningham and others, 1983; Steven and Morris, 1987).

Eruptions of crystal-rich ash-flow tuff from centers genetically related to the Bullion Canyon Volcanics (fig. 1) resulted in the formation of the Three Creeks caldera at 27.5 Ma (Steven, 1981), the Big John caldera at about 24 Ma (Steven, Cunningham, and Anderson, 1984), and the Monroe Peak caldera at 23 Ma (Rowley and others, 1988a,b). The Monroe Peak caldera is the largest caldera in the Marysvale volcanic field and was formed at the end of Bullion Canyon volcanism (Steven, Rowley, and Cunningham, 1984).

Isotopic data for Bullion Canyon Volcanics and related rocks (table 1, fig. 2) show a weak trend of increasing ε_{Nd} (–10 at 29 Ma to –5 at 21–22 Ma) with decreasing age. Initial strontium isotopic values are nearly constant ($^{87}Sr/^{86}Sr$=0.7052–0.7062), whereas Pb isotopic compositions are variable. With the exception of one sample obviously contaminated by upper crustal material (No. 78-958, initial $^{87}Sr/^{86}Sr$ = 0.716, $^{206}Pb/^{204}Pb$=19.8; table 1), Mount Dutton samples tend to have lower ε_{Nd} (–11) and $^{206}Pb/^{204}Pb$ (17.95–18.15), but similar initial $^{87}Sr/^{86}Sr$ to Bullion Canyon samples (fig. 2). Potassium, Rb, and U contents in samples from the Bullion Canyon Volcanics also increased with time, but remained relatively constant in Mount Dutton rocks.

At about 23–22 Ma, the composition of the igneous rocks changed to a bimodal suite of alkali rhyolite and basaltic rocks. These rocks are the products of the combined second and third igneous episodes, which continued to be erupted into the Quaternary. This change, from intermediate to bimodal volcanism at 23–22 Ma, is interpreted to be a result of the change from subduction to initial extension along the eastern margin of the Basin and Range province. The oldest basaltic lavas, erupted at 23–21 Ma (potassium-rich mafic lavas in table 1), contain 3.85 to 4.07 weight percent K_2O and have initial $^{87}Sr/^{86}Sr$ =0.7057–0.7061, ε_{Nd} = –6.7 to –8.5, and $^{206}Pb/^{204}Pb$=18.47–19.03. The high initial $^{87}Sr/^{86}Sr$ and low ε_{Nd} of these samples relative to similar age Bullion Canyon samples may reflect either crustal contamination or input from a subducted slab (Best and others, 1980; Walker and others, 1991).

Voluminous but locally erupted rhyolites were prevalent during the second and third episodes, from 22 to 14 Ma and from 9 to 5 Ma. The largest volume of alkali rhyolite,

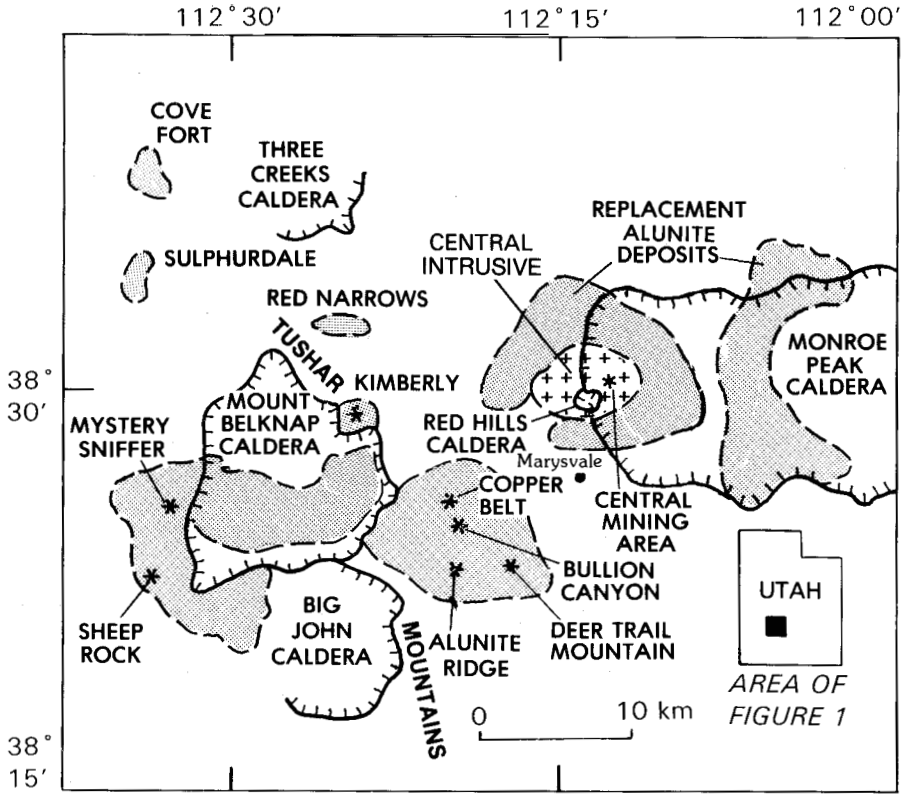

Figure 1. Location of calderas in central part of Marysvale volcanic field, Utah. Also shown are areas of altered rocks (shaded) and significant mineral deposits.

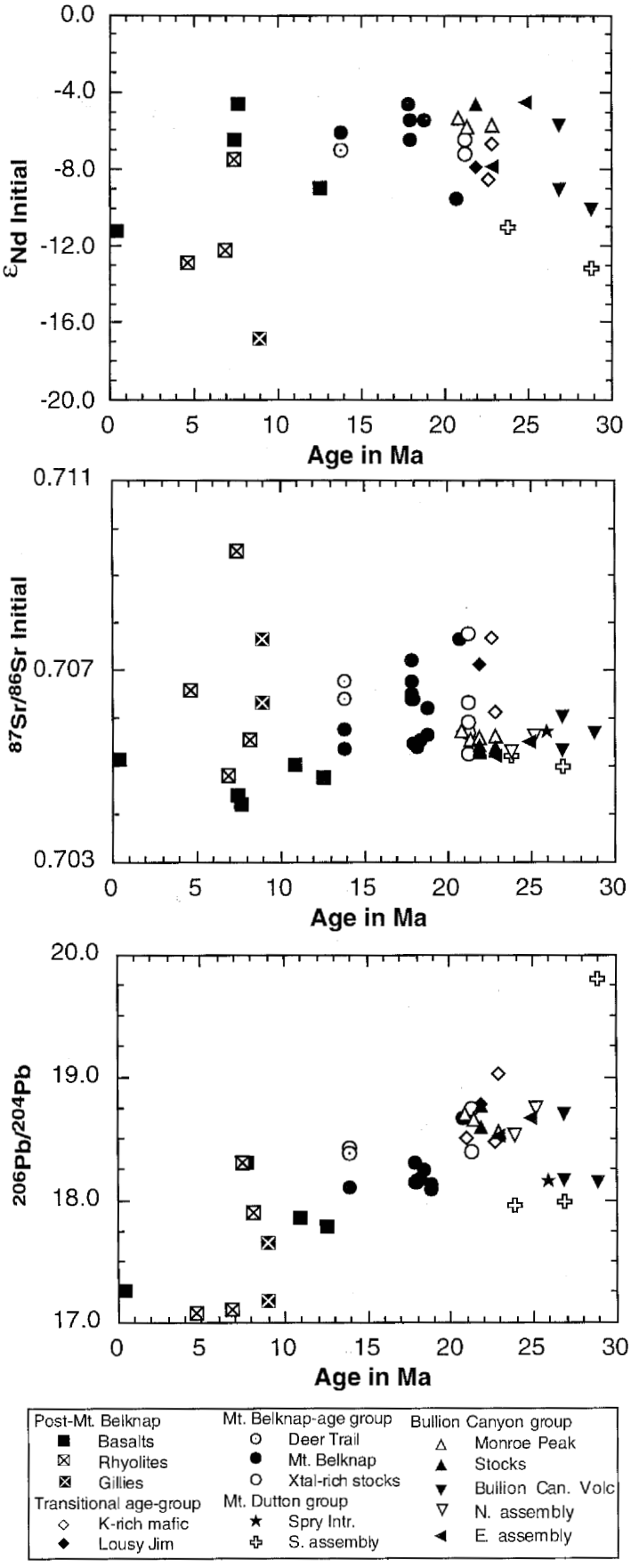

Figure 2. Plots of initial ε_{Nd}, $^{87}Sr/^{86}Sr$, and $^{206}Pb/^{204}Pb$ as functions of age for Marysvale samples.

called the Mount Belknap Volcanics (Cunningham and Steven, 1979; Budding and others, 1987), was erupted during the second episode (22–14 Ma, table 1). The Mount Belknap Volcanics was erupted from two areas (fig. 1): (1) the Mount Belknap caldera in the west, which formed at 19 Ma, and (2) a 12×12-km area, about 20 km east of the Mount Belknap caldera, that was active between 21 Ma at the northeast end of the area and 14 Ma at the southwest end (Cunningham and others, 1982).

The Mount Belknap Volcanics have higher silica contents (71.4–76.8 weight percent) than the older Bullion Canyon Volcanics (58.1–65.7 weight percent; table 1), as well as generally higher Rb contents (269–564 ppm) and lower Sr contents (23–100 ppm) than most of the Bullion Canyon Volcanics (69–142 ppm Rb, 473–928 ppm Sr).

The Mount Belknap Volcanics, in addition to having major-element compositions that contrast with the Bullion Canyon Volcanics and Mount Dutton Formation, have ε_{Nd} values similar to the latest Bullion Canyon Volcanics and among the highest ε_{Nd} values (–4.6 to –6.7, with one outlier; table 1, fig. 2) of any of the samples analyzed in this study. These data suggest that the processes involved in the production of these rhyolites involved comparatively little crustal contamination. Lead isotopic compositions of these samples (again with one exception) are tightly clustered with $^{206}Pb/^{204}Pb$=18.08–18.24 (table 1; fig. 2). In contrast, the initial $^{87}Sr/^{86}Sr$ values of the Mount Belknap Volcanics (0.7053–0.7072) are somewhat higher and more variable than those of the Bullion Canyon Volcanics (fig. 2). Because the Sr abundances of the Mount Belknap Volcanics are comparatively low, the Sr isotopic compositions of these samples were more susceptible to modification by relatively small amounts of crustal contamination than were those rocks of Bullion Canyon Volcanics, which have higher Sr contents.

During the third episode of igneous activity (9–5 Ma), sparse basaltic lavas had normal K_2O contents (1.82–2.97 weight percent), lower initial $^{87}Sr/^{86}Sr$ (0.7042–0.7051), highly variable ε_{Nd} (–4.7 to –11.2), and low but variable $^{206}Pb/^{204}Pb$ (17.3–18.3, table 1; fig. 2) when compared to the older, potassium-rich, basaltic lavas. Low initial Sr values in association with low ε_{Nd} and low $^{206}Pb/^{204}Pb$ have also been found among some late Tertiary basalt and basaltic andesite on the Markagunt Plateau approximately 80 km south of this study area (fig. 3), also along the western margin of the Colorado Plateau, by Nealey and others (in press). Although we have a rather limited data set, we note that the lowest $^{206}Pb/^{204}Pb$ and ε_{Nd} values are found in the sample (79-S-44) with the highest silica content, whereas the highest values are found in the only true basalt analyzed (78-164). This situation is analogous to that observed by

Table 1. Lead, Sr and Nd isotopic compositions of selected samples from the Marysvale Volcanic Field.

Sample	age (Ma)	SiO_2	206Pb[1] 204Pb	207Pb[1] 204Pb	208Pb[1] 204Pb	87Rb 86Sr	87Sr[2] 86Sr	87Sr 86Sr Ini.	147Sm 144Nd	143Nd[3] 144Nd	143Nd 144Nd Ini.	ε_{Nd} I
Basaltic lavas												
79-S-44	0.5	56.73	17.259	15.489	37.439	0.250	0.705122	0.70512	0.0998	0.512060	0.512060	-11.23
M848	7.6	55.12	18.302	15.589	37.434	0.257	0.704388	0.70436	0.1112	0.512297	0.512291	-6.53
78-164	7.8	48.65	18.297	15.568	37.907	0.230	0.704195	0.70417	0.1033	0.512390	0.512385	-4.71
M673	11	56.11	17.848	15.519	37.765	0.105	0.705026	0.70501				
M800	12.7	54.87	17.783	15.508	37.489	0.098	0.704748	0.70473	0.0914	0.512167	0.512159	-8.98
Rhyolites												
78-115	4.8	76.49	17.073	15.449	36.925	42.440	0.709433	0.7065	0.2048	0.511973	0.511967	-12.94
78-732	7	66.85	17.103	15.439	36.972	0.290	0.704789	0.70476	0.0985	0.512002	0.511997	-12.28
78-175	7.6	75.99	18.303	15.579	37.655	35.580	0.713320	0.7095	0.1134	0.512244	0.512238	-7.57
78-1695A	8.3	75.17	17.888	15.519	37.676	8.270	0.706495	0.70552				
Gillies Hill												
79-S-8A	9.1	69.61	17.171	15.479	37.652	0.919	0.707749	0.70763	0.0892	0.511762	0.511757	-16.92
79-S-9A	9.1	77.84	17.650	15.499	37.576	14.800	0.708223	0.70631				
MT. BELKNAP-AGE GROUP												
Deer Trail Rhyolite												
M945	14	73.2	18.417	15.586	38.537	0.628	0.706864	0.70674	0.0868	0.512296	0.512288	-6.43
Alunite												
M341	14	--	18.377	15.571	38.332	0.008	0.706362	0.70636	0.0503	0.512259	0.512254	-7.09
Mt. Belknap Volcanics												
M779A	14	76.15	18.097	15.568	38.080	24.120	0.710116	0.7053	0.1094	0.512315	0.512305	-6.11
M779B	14	75.31				23.300	0.710383	0.7058				
M687A	18	76.7	18.135	15.567	38.074	13.080	0.709814	0.70647				
M840A	18	76.54	18.303	15.596	38.371	45.230	0.717922	0.7064	0.1369	0.512391	0.512375	-4.64
M19A	18	75.64				24.340	0.712962	0.7067				
M672A	18.5	71.44	18.239	15.577	38.248	6.807	0.707308	0.70552				
M408A	18.1	76.76	18.143	15.567	38.234	1.945	0.706880	0.70638	0.0937	0.512290	0.512279	-6.51
M841	18	75.68				33.610	0.715782	0.7072				
M502A	18.1	76.04	18.148	15.567	38.149	15.350	0.709396	0.70545	0.1091	0.512344	0.512331	-5.49
M833	18.3	76.03	18.165	15.567	38.076	19.120	0.710339	0.70537				
M820A	19	75.77	18.123	15.566	38.085	18.750	0.710689	0.70563	0.0965	0.512343	0.512331	-5.47
M119A	19	76.41	18.075	15.577	38.107	20.730	0.711794	0.7062				
M50	20.9	71.5	18.662	15.638	38.999	5.180	0.709188	0.70765	0.1028	0.512131	0.512117	-9.60
Crystal-rich stocks												
M49A	21.4	74.45	18.380	15.605	38.494	2.293	0.705907	0.70521	0.0972	0.512251	0.512237	-7.24
M837A	21.4	74.76				11.060	0.709031	0.70567				
M837B	21.4	76.52				14.670	0.712219	0.70776				
M838A	21.4	74.26	18.730	15.623	38.910	5.280	0.707505	0.70590	0.1013	0.512287	0.512273	-6.55
M838B	21.4	76.62				17.730	0.711689	0.70630				
TRANSITIONAL-AGE GROUP												
K-rich mafic lavas												
M798	21.1	52.11	18.502	15.607	38.226	0.215	0.705754	0.70569				
M657	22.8	58.07	18.469	15.617	38.506	0.326	0.707785	0.70768	0.1171	0.512187	0.512170	-8.53
M856	23	53.39	19.027	15.667	39.001	0.220	0.706182	0.70611	0.1031	0.512278	0.512262	-6.71
Lousy Jim												
M822	22	69.4				1.991	0.707752	0.70713				
M823A	22	67.2	18.775	15.664	38.876	2.671	0.707955	0.70712	0.1041	0.512217	0.512202	-7.91
BULLION CANYON VOLCANICS AND RELATED ROCKS												
Monroe Peak												
M678	21	62.83	18.694	15.626	38.559	0.626	0.705887	0.70570	0.1052	0.512345	0.512331	-5.43
79-1664A	23	65.74	18.551	15.624	38.410	1.897	0.706210	0.70559	0.1016	0.512327	0.512312	-5.75
M569	21.5	64.87	18.640	15.626	38.446	1.448	0.705962	0.70552	0.0937	0.512319	0.512306	-5.90
M608	22	65.7				1.533	0.706049	0.70557				
Monzonite stocks												
M867	22	58.25	18.583	15.614	38.430	0.949	0.705566	0.70527				
M621	22	58.58	18.758	15.582	38.521	0.841	0.705583	0.70532	0.1060	0.512386	0.512308	-4.62
M845	22	59.58				1.238	0.705807	0.70542				
M851	22	58.69				0.941	0.705574	0.70528				
M869	23	58.1				0.833	0.705552	0.70528				
M870	23	58.67				0.945	0.705659	0.70535				
Bullion Canyon Volcanics												
M90	27	64.08	18.161	15.586	38.343	0.381	0.706156	0.70601	0.1026	0.512152	0.512134	-9.12
79-1666	27	60.43	18.685	15.655	38.366	0.557	0.705493	0.70528	0.1035	0.512322	0.512304	-5.80
79-S-1	29	61.89	18.146	15.577	38.088	0.190	0.705728	0.70565	0.1084	0.512100	0.512079	-10.14
Northern Assemblage												
79-S-3	24	55.91	18.513	15.617	38.154	0.302	0.705353	0.70525				
M739	25.3	61.75	18.736	15.616	38.163	0.830	0.705898	0.70560				
Eastern Assemblage												
79-1517	23	56.56	18.523	15.588	38.260	0.170	0.705255	0.70520	0.1052	0.512215	0.512199	-7.94
79-1518	25	58.74	18.661	15.616	38.232	0.350	0.705614	0.70549	0.1079	0.512388	0.512370	-4.55
MOUNT DUTTON FMN. AND RELATED ROCKS												
Mount Dutton Fmn. (southern assemblage)												
79-1665	24	56.55	17.953	15.558	38.324	0.151	0.705241	0.70519	0.1060	0.512056	0.512039	-11.04
78-698	27	59.33	17.987	15.548	38.171	0.343	0.705092	0.70496				
78-958	29	57.51	19.796	15.787	39.983	0.850	0.716530	0.71618	0.1216	0.511945	0.511922	-13.20
Spry Intrusion												
R2106	26.1	66.73	18.152	15.549	38.148	0.360	0.705833	0.70570				

[1] Corrected for mass fractionation during analyses of 0.12 ± 0.03% per mass based on analyses of Pb standard SRM-981. Uncertainties in the data generally correspond to the fractionation uncertainties.

[2] Measured uncertainties are generally 0.003% to 0.004% and are relative to a value of 0.710254 ± 15 (6 analyses) of Sr standard SRM-987.

[3] Measured uncertainties are generally 0.003% to 0.004% and are relative to a value of 0.511854 ± 12 (8 analyses) of the La Jolla Nd Standard.

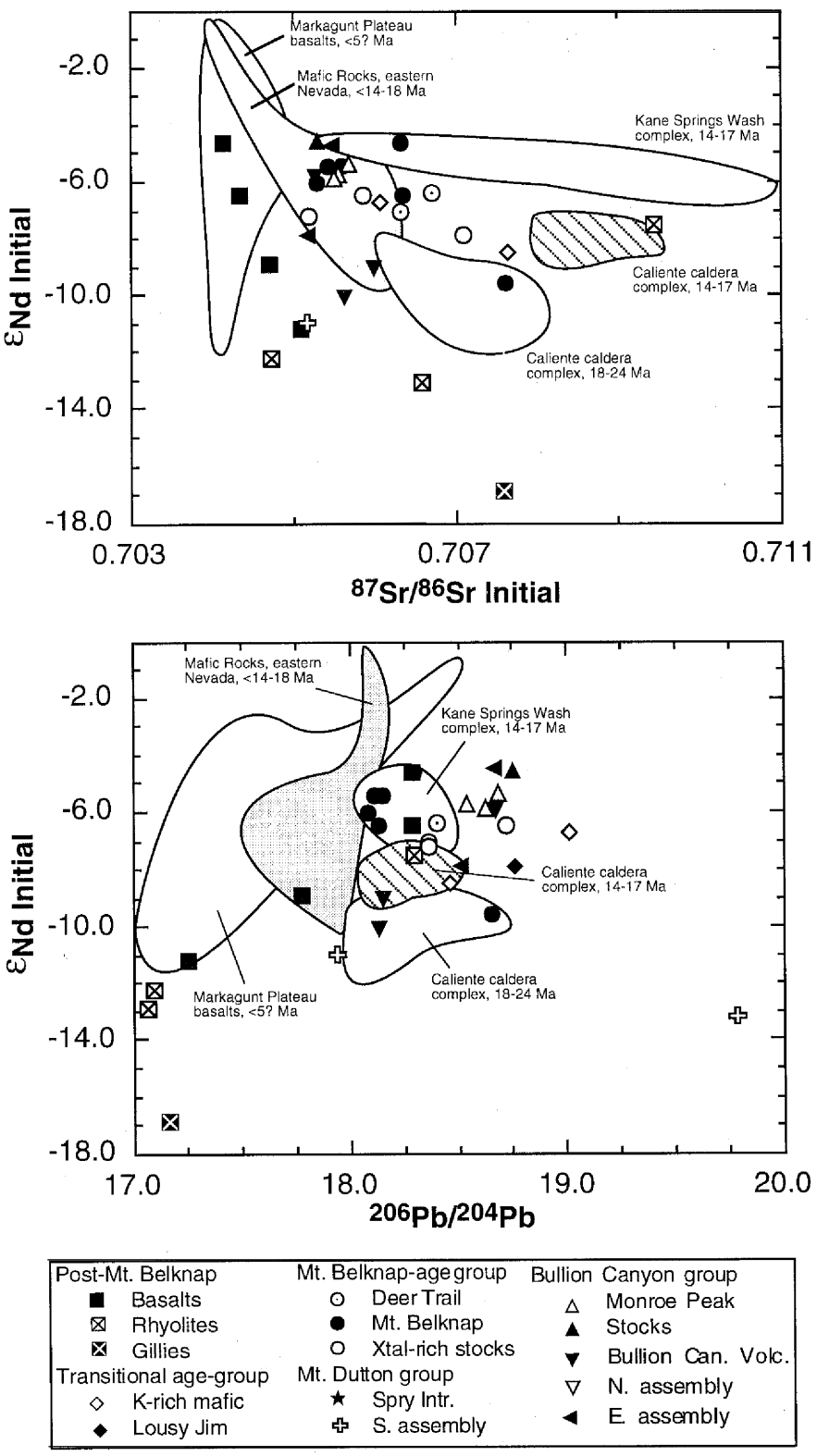

Figure 3. Plots of ε_{Nd} vs. $^{87}Sr/^{86}Sr$, and $^{206}Pb/^{204}Pb$ for Marysvale samples. Shown for reference are fields of data for the Kane Springs Wash and Caliente caldera complexes in southeastern Nevada and the Markagunt Plateau in southwestern Utah.

Nealey and others (in press), who ascribed this rather unusual isotopic signature to interaction of ascending mantle-derived magmas with the lower crust. This interpretation was based primarily on two factors: (1) a suite of deep-crustal xenoliths from the San Francisco volcanic field, central Arizona (along the southern margin of the Colorado Plateau) have isotopic characteristics that represent the end-member of this trend ($^{206}Pb/^{204}Pb \approx 16.0$, $^{87}Sr/^{86}Sr \approx 0.7025$, $\varepsilon_{Nd} \approx -20$; Nealey and Unruh, 1991), and (2) evidence for this isotopic signature is not found west of the approximate Colorado Plateau

boundary, even among similar-aged basalts in the St. George basin immediately southwest of the Markagunt Plateau (Unruh and others, in press).

Rhyolites that were erupted during the third episode of igneous activity had major-element compositions similar to those of the 22–14 Ma group but had markedly different radiogenic-isotope characteristics. Lead, Sr, and Nd isotopic ratios all show much more variation than ratios observed among the other age groups (fig. 2), and the lowest ε_{Nd} values(–12 to –16) and $^{206}Pb/^{204}Pb$ (17.0–17.2) are found among these samples. However, initial $^{87}Sr/^{86}Sr$ values do not appear to be well correlated with Nd or Pb isotopic compositions (figs. 2 and 3), and rhyolites from the third episode show the widest variation in initial Sr and Nd values found within the entire sample suite (again with the exception of the highly contaminated Mount Dutton sample previously mentioned).

The isotopic trends exhibited by the Bullion Canyon and Mount Belknap Volcanics show similarities to those exhibited by the similar-age Caliente and Kane Springs Wash caldera complexes in southeastern Nevada (fig. 3; data from Scott and others, 1995; Unruh and others, 1995; D.M. Unruh, unpub. data, 1995). In both areas, ε_{Nd} values generally increase with decreasing age (at least from 29–18 Ma in Marysvale), whereas initial $^{87}Sr/^{86}Sr$ values tend to become more variable with decreasing age (figs. 2 and 3). In both areas these features may be attributed to different processes and sources involved during the change from subduction-related to extension-related volcanism. In the Caliente and Kane Springs Wash complexes, this transition is also reflected in the major-element chemistry of the rhyolite tuffs: Kane Springs Wash and post-17 Ma Caliente tuffs become metaluminous to weakly peralkaline, whereas the older tuffs are generally peraluminous (Rowley and others, 1995; Scott and others, 1995).

The Mount Belknap and Bullion Canyon Volcanics show a larger range of Pb isotopic compositions than do the tuffs of the Caliente and Kane Springs Wash complexes (figs. 3 and 4), although Pb isotopic data for the individual groups show fairly tight clusters (fig. 4). Lead isotopic data for the post-Mount Belknap samples are more similar to those for late Tertiary Markagunt Plateau basalts than to data for either Marysvale or Caliente-Kane Springs Wash samples.

All of the data on the $^{206}Pb/^{204}Pb$ vs. $^{207}Pb/^{204}Pb$ diagram plot significantly above the "northern hemisphere reference line" (NHRL; Hart, 1984), that represents the average trend of oceanic basalts in the northern hemisphere. This suggests that the Pb isotopic characteristics of these samples are derived primarily from lithospheric sources. Furthermore, Pb isotopic data for Marysvale samples in general show a pronounced average decrease in $^{206}Pb/^{204}Pb$ with decreasing age from about 22 Ma to the present (fig. 2), which may indicate a progressive change in the source region for these samples. A best-fit line through the $^{206}Pb/^{204}Pb$ vs. $^{207}Pb/^{204}Pb$ data in figure 4 yields an apparent age of 1.9 in view of the evidence for multiple sources for these samples, this apparent age may have no rigorous significance.

The isotopic data presented here for Marysvale samples are consistent with an interpretation of having been derived from three primary sources: the lithospheric mantle (his context, the terms "upper" and "lower" crust are not meant to imply that these represent exactly two discreet physical entities; rather, these terms are used in the context of two end-member isotopic signatures). The upper-crustal end-member, most evident in Mount Dutton sample 78-958 (table 1), is characterized by radiogenic Pb and Sr ($^{206}Pb/^{204}Pb>19.8$; $^{87}Sr/^{86}Sr>0.715$) and nonradiogenic Nd ($\varepsilon_{Nd}<-13$). The lower-crustal end-member, most evident in Gillies Hill sample 79-S8A, is also characterized by low ε_{Nd} (<-18) but perhaps only moderately radiogenic Sr ($^{87}Sr/^{86}Sr>0.708$) and nonradiogenic Pb ($^{206}Pb/^{204}Pb<17.0$). This lower-crustal end-member is similar to that inferred for the Markagunt Plateau except that Sr appears to have been more radiogenic in the Marysvale area.

The isotopic characteristics of the lithospheric mantle are probably most-closely approximated by the only true basalt analyzed (sample 78-164, table 1; $\varepsilon_{Nd} \approx -4.7$, $^{206}Pb/^{204}Pb \approx 18.3$, and $^{87}Sr/^{86}Sr \approx 0.704$). These values are very similar to those estimated for the lithospheric mantle under the Kane Springs Wash and Caliente caldera complexes (Scott and others, 1995; Unruh and others, 1995), and surprisingly close to those estimated by Johnson and Thompson (1991; $\varepsilon_{Nd} \approx -4$, $^{206}Pb/^{204}Pb \approx 18.2$, $^{87}Sr/^{86}Sr \approx 0.705$) for the isotopic composition of the lithospheric mantle in the northern Rio Grande Rift on the opposite side of the Colorado Plateau. This isotopic component may represent the lithospheric mantle directly or the lithospheric mantle modified by a "subduction component" (Fitton and others, 1991) in the form of fluids or melts derived from the subducted slab. The fact that basalts with $\varepsilon_{Nd} = -4$ to 0 are relatively common among late Tertiary and Quaternary basalts on the Markagunt Plateau (Nealey and others, in press) suggests that the ε_{Nd} value of unmodified lithosphere in this area may be closer to zero (Farmer and others, 1989).

During eruption of the Mount Dutton Formation, the Bullion Canyon Volcanics, and the 20–18 Ma Mount Belknap Volcanics, crustal interaction progressively decreased, as evidenced by progressively increasing ε_{Nd} (fig. 2). The variation in Pb isotopic data during this interval suggests that both the Bullion Canyon and Mount Dutton magmas interacted with both upper and lower crust (figs. 2 and 3). The apparent progressive decrease in crustal interaction may reflect either thinning of the lithosphere during the onset of extension, providing a thinner column of crust for rising magmas to interact with, or production of progressively larger volumes of magma within the lithospheric mantle: all of these in effect dilute the crustal influence.

The similarity of neodymium, lead, and strontium isotopic values, together with the contrasting major element

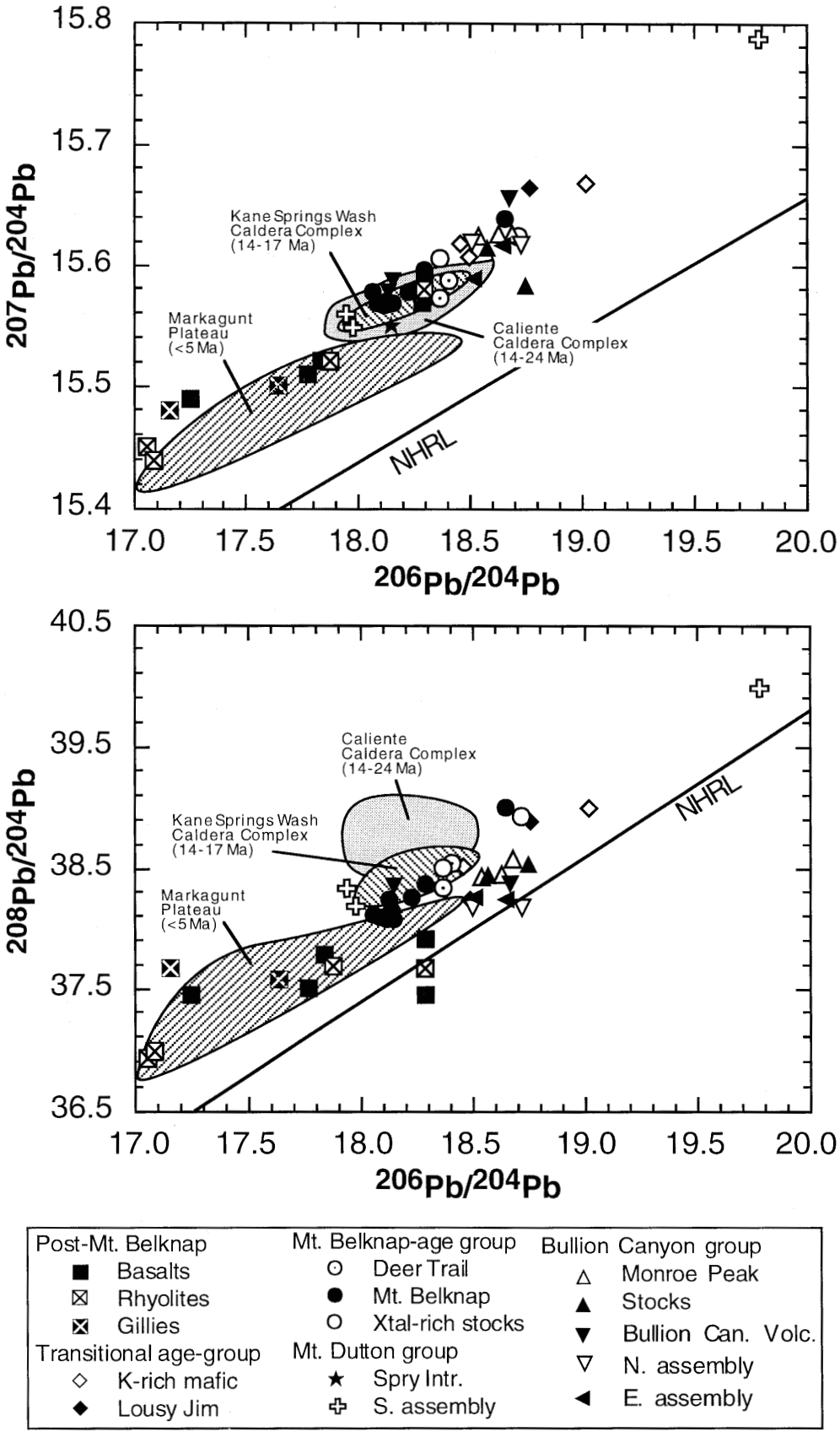

Figure 4. $^{207}Pb/^{204}Pb$ and $^{208}Pb/^{204}Pb$ vs. $^{206}Pb/^{204}Pb$ diagrams for Marysvale samples. Shown for reference are fields of data for the Kane Springs Wash and Caliente caldera complexes in southeastern Nevada and the Markagunt Plateau in southwestern Utah.

compositions, between the latest Bullion Canyon Volcanics (Monroe Peak caldera) and the spatially related early Mount Belknap Volcanics (crystal-rich stocks), is consistent with the interpretation that the Mount Belknap Volcanics was

derived from partial melting of Bullion Canyon batholithic rocks. This could be achieved as rising isotherms from the onset of extensional tectonics melted nearly eutectic magmas from the former magma chambers that fed Bullion Canyon volcanoes.

The Sr, Nd (fig. 3), and particularly the Pb isotopic compositions (fig. 4) of the samples formed during the third episode of volcanic activity appear to be strongly influenced by interaction with the lower crust (although rhyolites from this group have highly variable isotopic compositions). The fact that both mafic and silicic rocks have this signature may imply that the site of primary melt generation may have risen to the crust-mantle boundary during this period, particularly if this boundary had been modified by numerous earlier injections of mantle-derived magmas (Johnson and others, 1990). This interpretation is consistent with episodic intervals of increased extension and derivation of the late rhyolitic magmas from a variety of levels in the crust as isotherms rose in response to extension .

REFERENCES CITED

Best, M.G., McKee, E.H., and Damon, P.E., 1980, Space-time-composition patterns of late Cenozoic mafic volcanism, southwestern Utah and adjoining areas: American Journal of Science, v. 180, p. 1035–1050.

Budding, K.E., Cunningham, C.G., Zielinski, R.A., Steven, T.A., and Stern, C.R., 1987, Petrology and chemistry of the Joe Lott Tuff Member of the Mount Belknap Volcanics, Marysvale volcanic field, west-central Utah: U.S. Geological Survey Professional Paper 1354, 47 p.

Cunningham, C.G., Ludwig, K.R., Naeser, C.W., Weiland, E.K., Mehnert, H.H., Steven, T.A., and Rasmussen, J.D., 1982, Geochronology of hydrothermal uranium deposits and associated igneous rocks in the eastern source area of the Mount Belknap Volcanics, Marysvale, Utah: Economic Geology, v. 77, no. 2, p. 444–454.

Cunningham, C.G., and Steven, T.A., 1979, Mount Belknap and Red Hills calderas and associated rocks, Marysvale volcanic field, west-central Utah: U.S. Geological Survey Bulletin 1468, 34 p.

Cunningham, C.G., Steven, T.A., Rowley, P.D., Glassgold, L.B., and Anderson, J.J., 1983, Geologic map of the Tushar Mountains and adjoining areas, Marysvale volcanic field, Utah: U.S. Geological Survey Miscellaneous Investigations Series Map I–1430–A, scale 1:50,000.

Farmer, G.L., Perry, F.V., Semken, S., Crowe, B., Curtis, D., and DePaolo, D.J., 1989, Isotopic evidence on the structure and origin of subcontinental lithospheric mantle in southern Nevada: Journal of Geophysical Research, v. 94, p. 7885–7898.

Fitton, J.G., James, D., and Leeman, W.P., 1991, Basic magmatism associated with Late Cenozoic extension in the western United States—Compositional variations in space and time: Journal of Geophysical Research, v.96, p. 13693–13711.

Hart, S.R., 1984, A large-scale isotope anomaly in the Southern Hemisphere mantle: Nature, v. 309, p. 753–757.

Johnson, C.M. and Thompson, R.A., 1991, Isotopic composition of Oligocene mafic volcanic rocks in the northern Rio Grande rift; evidence for contributions of intraplate and subduction magmatism to the evolution of the lithosphere: Journal of Geophysical Research, v. 96, p. 13593–13608.

Johnson, C.M., Lipman, P.W., and Czamanske, G.K., 1990, H, O, Sr, Nd, and Pb isotope geochemistry of the Latir volcanic field and cogenetic intrusions, New Mexico, and relations between evolution of a continental magmatic center and modifications of the lithosphere: Contributions to Mineralogy and Petrology, v. 104, p. 99–124.

Nealey, L.D. and Unruh, D.M., 1991, Geochemistry and isotopic characteristics of deep crustal xenoliths from Tule Tank, San Francisco Volcanic Field, northern Arizona: Arizona Geological Society Digest, v. 19, p. 153–163.

Nealey, L.D., Unruh, D.M., and Maldonado, F., in press Sr, Nd, and Pb isotopic maps of Pleistocene and Holocene volcanic rocks of the Panguitch 30' × 60' quadrangle, southwest Utah: U.S. Geological Survey Open-File Report, scale 1:250,000.

Rowley, P.D., Cunningham, C.G., Steven, T.A., and Naeser, C.W., 1988a, Geologic map of the Marysvale quadrangle, Piute County, Utah: Utah Geological and Mineral Survey Map 105, 15 p., scale 1:24,000.

_____1988b, Geologic map of the Antelope Range quadrangle, Sevier and Piute Counties, Utah: Utah Geological and Mineral Survey Map 106, 14 p., scale 1:24,000.

Rowley, P.D., Mehnert, H.H., Naeser, C.W., Snee, L.W., Cunningham, C.G., Steven, T.A., Anderson, J.J., Sable, E.G., and Anderson, R.E., 1994, Isotopic ages and stratigraphy of Cenozoic rocks of the Marysvale volcanic field and adjacent areas, west-central Utah: U.S. Geological Survey Bulletin 2071, 35 p.

Rowley, P.D., Nealey, L.D., Unruh, D.M., Snee, L.W., Mehnert, H.H., Anderson, R.E., Gromme, S.C., and Siders, M.A., 1995, Stratigraphy of Oligocene and Miocene ash-flow tuffs in and near the Caliente caldera complex, southeastern Nevada and southwestern Utah, *in* Scott, R.B., and Swadley, W C, eds., Geologic studies in the Basin and Range to Colorado Plateau transition in southeastern Nevada, southwestern Utah, and northwestern Arizona: U.S. Geological Survey Bulletin 2056–B, p. 47–88.

Rowley, P.D., Steven, T.A., Anderson, J.J., and Cunningham, C.G., 1979, Cenozoic stratigraphic and structural framework of southwestern Utah: U.S. Geological Survey Professional Paper 1149, 22 p.

Scott, R.B., Unruh, D.M., Snee, L.W., Harding, A.E., Blank, H.R. Jr., Budahn, J.R., and Mehnert, H.H., 1995, Relation of peralkaline magmatism to heterogeneous extension during the middle Miocene, southeastern Nevada: Journal of Geophysical Research, v. 100, p. 10381–10401.

Steven, T.A., 1981, Three Creeks caldera, southern Pavant Range, Utah: Brigham Young University Geology Studies, v. 28, pt. 3, p. 1–7.

Steven, T.A., Cunningham, C.G., and Anderson, J.J., 1984, Geologic history and uranium potential of the Big John caldera, southern Tushar Mountains, Utah, *in* Steven, T.A., ed., Igneous activity and related ore deposits in the western and southern Tushar Mountains, Marysvale volcanic field, west-central Utah: U.S. Geological Survey Professional Paper 1299–B, p. 23–33.

Steven, T.A., Cunningham, C.G., Naeser, C.W., and Mehnert, H.H., 1979, Revised stratigraphy and radiometric ages of volcanic rocks and mineral deposits in the Marysvale area, west-central Utah: U.S. Geological Survey Bulletin 1469, 40 p.

Steven, T.A., and Morris, H.T., 1987, Summary mineral resource appraisal of the Richfield 1° × 2° quadrangle, west-central Utah: U.S. Geological Survey Circular 916, 24 p.

Steven, T.A., Morris, H.T., and Rowley, P.D., 1990, Geologic map of the Richfield 1˚ × 2˚ quadrangle, west-central Utah: U.S. Geological Survey Miscellaneous Investigations Series Map I–1901, scale 1:250,000.

Steven, T.A., Rowley, P.D., and Cunningham, C.G., 1984, Calderas of the Marysvale volcanic field, west-central Utah: Journal of Geophysical Research, v. 89, no. B10, p. 8751-8764.

Unruh, D.M., Nealey, L.D., Rowley, P.D., Snee, L.W., Mehnert, H.H., and Anderson, R.E., 1995, Strontium and neodymium isotopic survey and ash-flow tuffs and related rocks from the Caliente caldera complex, southeastern Nevada and southwestern Utah, *in* Scott, R.B., and Swadley, W C, eds., Geologic studies in the Basin and Range to Colorado Plateau transition in southeastern Nevada, southwestern Utah, and northeastern Arizona: U.S. Geological Survey Bulletin 2056–D, p. 113–129.

Unruh, D.M., Nealey, L.D., and Maldonado, Florian, in press, Sr-Nd-Pb isotopic maps of late Cenozoic volcanic rocks of the St. George 30' × 60' quadrangle, southwest Utah: U.S. Geological Survey Open-File Report, scale 1:250,000.

Walker, J.A., Mattox, S.R., and Feigenson, M.D., 1991, Temporal changes in the source region of Cenozoic lavas of the Utah transition zone: Geological Society of America Abstracts with Programs, v. 23, no. 4, p. 102.

Next section →